Research Square

Preprints are preliminary reports that have not undergone peer review.
They should not be considered conclusive, used to inform clinical practice,
or referenced by the media as validated information.

Purely Bianisotropic Response in Loss-Compensated Plasmonic Nanodimers

Mohammad Shoai
Iran University of Science and Technology
Amir Saman Nooramin
a_nooramin@iust.ac.ir
Iran University of Science and Technology
Homayoon Oraizi
Iran University of Science and Technology

Article

Keywords: Bianisotropic scatterer, plasmonic nanodimer, loss compensation, directional scattering

Posted Date: November 12th, 2026

DOI: https://doi.org/10.21203/rs.3.rs-10682384/v1

License: This work is licensed under a Creative Commons Attribution 4.0 International License.
Read Full License

Additional Declarations: No competing interests reported.

Purely Bianisotropic Response in Loss-Compensated Plasmonic Nanodimers

Mohammad Shoai[1], Amir Saman Nooramin[1,✉] & Homayoon Oraizi[1]

[1]School of Electrical Engineering, Iran University of Science and Technology, Tehran 1684613114, Iran. ✉email: a_nooramin@iust.ac.ir

A purely bianisotropic response is characterized by the complete suppression of a scatterer's direct electric and magnetic responses, while the indirect magnetoelectric and electromagnetic ones remain finite. Such a response is fundamentally forbidden in passive reciprocal systems by the optical theorem. In this work, we derive a generalized condition showing that this regime becomes accessible in reciprocal lossy scatterers when dissipative and radiative losses are fully compensated, thereby extending the concept of purely bianisotropic scattering beyond the limits of passivity. As a physical realization, we propose a loss-compensated plasmonic nanoshell dimer consisting of two geometrically asymmetric silver nanoshells with gain-doped silica cores. The detuned plasmonic resonances suppress the net electric dipole response, while optical gain compensates losses, resulting in a nearly pure bianisotropic response in which the magnetoelectric polarizabilities exceed the direct electric and magnetic polarizabilities by more than two orders of magnitude. We further demonstrate that this regime enables unconventional scattering phenomena, including forward-scattering suppression (the second Kerker effect) and lateral scattering. Moreover, introducing a passive nanoshell between the two gain-assisted particles transforms the lateral scattering into highly directional scattering through magnetoelectric interference.

Keywords Bianisotropic scatterer, plasmonic nanodimer, loss compensation, directional scattering

The electromagnetic response of a scatterer to an external excitation can be rigorously described through multipole expansion theory[1,2]. Within the dipole approximation, where higher-order multipole contributions are neglected, the scatterer's response is characterized by the induced electric dipole moment, $\boldsymbol{p}$, and magnetic dipole moment $\boldsymbol{m}$. For linear scatterers, these dipole moments are linearly related to the local electric and magnetic fields through the polarizability tensor $\bar{\bar{\boldsymbol{\alpha}}}$

$$\begin{pmatrix} p \\ m \end{pmatrix} = \bar{\bar{\alpha}} \begin{pmatrix} E_{loc} \\ H_{loc} \end{pmatrix}, \bar{\bar{\alpha}} = \begin{pmatrix} \bar{\bar{\alpha}}_{ee} & \bar{\bar{\alpha}}_{em} \\ \bar{\bar{\alpha}}_{me} & \bar{\bar{\alpha}}_{mm} \end{pmatrix} \tag{1}$$

The diagonal polarizability tensors, $\bar{\bar{\alpha}}_{ee}$ and $\bar{\bar{\alpha}}_{mm}$, describe the direct electric and magnetic responses of the scatterer to the corresponding fields, whereas the off-diagonal tensors (bianisotropy terms), $\bar{\bar{\alpha}}_{em}$ and $\bar{\bar{\alpha}}_{me}$, account for the indirect magnetoelectric and electromagnetic responses[3-5]. A particularly intriguing regime arises when the electric and magnetic polarizabilities vanish, i.e., $\bar{\bar{\alpha}}_{ee} = 0$, $\bar{\bar{\alpha}}_{mm} = 0$. In this limit, the scatterer's response is no longer characterized by direct dipole excitations. Instead, the interaction with the electromagnetic field is determined solely by the indirect magnetoelectric coupling tensors $\bar{\bar{\alpha}}_{em}$ and $\bar{\bar{\alpha}}_{me}$. Consequently, an incident electric field induces only magnetic dipole moments, whereas an incident magnetic field induces only electric dipole moments. Such a particle is referred to as a purely bianisotropic scatterer[6]. Under this condition, Eq. (1) reduces to

$$p = \bar{\bar{\alpha}}_{em}.H_{loc} \ , m = \bar{\bar{\alpha}}_{me}.E_{loc} \tag{2}$$

The purely bianisotropic condition described above represents an ideal limit in which the direct coupling coefficients vanish completely. However, the authors in[6] showed that a passive, lossless scatterer cannot achieve this ideal state. Under energy-conservation constraints, the indirect coupling coefficients are fundamentally bounded by the direct coupling terms. When either $\bar{\bar{\alpha}}_{ee} = 0$ or $\bar{\bar{\alpha}}_{mm} = 0$, the cross-coupling terms $\bar{\bar{\alpha}}_{em}$ and $\bar{\bar{\alpha}}_{me}$ must vanish identically. Nevertheless, their work demonstrated that no fundamental restriction exists on the relative strength of the magnetoelectric terms; consequently, a lossless scatterer can exhibit a nearly pure bianisotropic response when the indirect coupling coefficients dominate the direct ones. To realize this regime, they proposed a dimer of two closely spaced, subwavelength, lossless particles whose individual electric polarizabilities have real parts of equal magnitude but opposite signs. In this configuration, the induced electric dipole moments of the two particles cancel, $p_1 = -p_2$, strongly suppressing the direct electric response while preserving a finite magnetoelectric coupling. The proposed dimer consisted of two dielectric spheres, one of which possessed a negative real permittivity.

`

In[7], the authors aimed to design an overall lossless scatterer that exhibits a shadow-free response, an object characterized by a completely vanishing forward scattering amplitude while maintaining a non-zero total scattering cross-section. Although they initially explored parity-time (PT)-symmetric structures as candidates for realizing this effect, they demonstrated that standard PT-symmetric configurations are fundamentally unsuited for this purpose in unbounded space. They therefore turned their attention to the purely bianisotropic scatterer, as it serves as the underlying mechanism to realize a shadow-free response in an overall lossless system. To achieve this, they developed a generalized non-Hermitian microwave model consisting of two closely spaced short dipole antennas. By precisely tuning the lumped impedances loading each dipole element, they engineered dipole moments of equal magnitude but opposite sign, following the design methodology of[6] to induce a purely bianisotropic response. Achieving this regime required the real part of one dipole's load impedance to be negative, providing the amplification needed to balance both dissipative and radiative losses.

In this work, we propose an optical realization of a nearly pure bianisotropic scatterer based on a gain-assisted plasmonic nanoshell dimer. The structure consists of two geometrically asymmetric spherical nanoparticles, each comprising a gain-doped dielectric core surrounded by a metallic shell. Unlike the dielectric realization of[6], the proposed structure exploits asymmetric plasmonic nanoshells, leading to resonance detuning between the two particles. This detuning naturally yields electric polarizabilities with opposite signs, while preserving the structural asymmetry required to sustain a bianisotropic response. Furthermore, optical gain is introduced into the core of each nanoparticle to compensate for both dissipative and radiative losses in the system. As will be demonstrated, this loss-compensation mechanism is the key requirement for approaching a nearly pure bianisotropic regime in lossy systems. The use of asymmetric plasmonic dimers for realizing bianisotropic responses has been extensively studied[8,9]. Similarly, optical gain has been widely explored for loss compensation in plasmonic systems: it has been introduced into the core of plasmonic nanoshells to compensate intrinsic losses and enhance resonance quality[10], incorporated into chiral scatterers to enhance optical chirality[11], and employed in plasmonic nanoshell dimers to achieve strong near-field enhancement[12]. In the present work, we exploit this established loss-compensation mechanism for a different purpose: to realize a predominantly bianisotropic response, extending the concept to the optical regime through a realistic plasmonic platform and thereby accessing its associated unconventional scattering phenomena and wave-manipulation capabilities.

The paper is structured as follows. The fundamental polarizability constraints for lossy systems are first derived, establishing the loss-compensation condition as the key requirement for realizing a purely bianisotropic response. The design of a loss-compensated plasmonic nanoshell dimer is then presented, along with the numerical results confirming the nearly pure bianisotropic behavior. Subsequently, the experimental feasibility and resulting scattering phenomena of the proposed design are discussed. Finally, concluding remarks are provided.

Fundamental Constraints on the Polarizability Tensor of Lossy Scatterers

The polarizability tensor of a bianisotropic scatterer is not arbitrary but is constrained by fundamental physical principles. For linear, time-invariant systems in the absence of external bias, reciprocity imposes symmetry relations on the sub-blocks of the tensor. Specifically, the Onsager–Casimir relations require $\bar{\bar{\alpha}}_{ee} = \bar{\bar{\alpha}}_{ee}{}^{T}$, $\bar{\bar{\alpha}}_{mm} = \bar{\bar{\alpha}}_{mm}{}^{T}$, $\bar{\bar{\alpha}}_{em} = -\bar{\bar{\alpha}}_{me}{}^{T}$, where the superscript "T" denotes the transpose operation. The minus sign in the magnetoelectric relation follows from the odd parity of the magnetic field under time reversal. These constraints reduce the degrees of freedom of the polarizability tensor and must be satisfied by any reciprocal scatterer. Beyond reciprocity, energy conservation imposes more stringent constraints on the polarizability tensor. For a bianisotropic scatterer embedded in a homogeneous medium, the extinction power, defined as the time-averaged work done by the incident field E_{inc} and H_{inc} to drive p and m, can be written as[4,5]

$$P_{ext} = \frac{k}{2\eta}\,\mathrm{Im}\{F^{\dagger}\bar{\bar{\alpha}}F\} \tag{3}$$

where $F = (E_{inc} \quad H_{inc})^{T}$, k is the wavenumber in the host medium, η is the medium impedance, and subscript ''†'' denotes conjugate transpose operation. Moreover, the total power scattered by the induced dipoles can be expressed as

$$P_{sca} = \frac{k^4}{12\pi\eta}\left[F^{\dagger}\bar{\bar{\alpha}}^{\dagger}\bar{\bar{\alpha}}F\right] \tag{4}$$

For a passive scatterer, energy conservation requires that the extinction power equals the sum of the scattered and absorbed powers,

$$P_{ext} = P_{sca} + P_{abs} \tag{5}$$

`

where ($P_{abs} \geq 0$). Substituting Eqs. (3) and (4) into Eq. (5) yields the optical theorem for a passive lossy scatterer.

$$\mathrm{Im}\{F^{\dagger}\bar{\bar{\alpha}}F\} \geq \frac{k^3}{6\pi}[F^{\dagger}\bar{\bar{\alpha}}^{\dagger}\bar{\bar{\alpha}}F] \tag{6}$$

With strict equality for lossless scatterers ($P_{abs} = 0$). In this work, $\bar{\bar{\alpha}}$ denotes the full electrodynamic polarizability tensor, including radiation-reaction corrections, rather than the quasistatic polarizability, which does not generally satisfy the optical theorem in Eq. (6). To investigate the implications of passivity in the purely bianisotropic regime, defined by $\bar{\bar{\alpha}}_{ee} = \bar{\bar{\alpha}}_{mm} = 0$, we consider plane-wave illumination. Under these conditions, the extinction power in Eq. (3) reduces to

$$P_{ext} = \frac{k}{2\eta}\mathrm{Im}\{E_{inc}^{\dagger}\bar{\bar{\alpha}}_{em}H_{inc} + H_{inc}^{\dagger}\bar{\bar{\alpha}}_{me}E_{inc}\} \tag{7}$$

For a reciprocal scatterer satisfying $\bar{\bar{\alpha}}_{em} = -\bar{\bar{\alpha}}_{me}{}^{T}$, the magnetoelectric contributions cancel under plane-wave illumination, yielding $P_{ext} = 0$. Consequently, the left-hand side of Eq. (6) vanishes. In contrast, the right-hand side contains the positive-semidefinite quadratic form $\bar{\bar{\alpha}}^{\dagger}\bar{\bar{\alpha}}$, which is nonzero whenever the magnetoelectric/electromagnetic polarizabilities are finite. Therefore, for a passive system, the inequality can be satisfied only if $\bar{\bar{\alpha}}_{em} = \bar{\bar{\alpha}}_{me} = 0$. This result demonstrates that a nontrivial purely bianisotropic response is incompatible with the simultaneous enforcement of passivity and reciprocity. Consequently, the realization of an ideal purely bianisotropic scatterer requires the relaxation of at least one of these constraints. In this work, we relax the passivity condition by introducing optical gain ($P_{abs} < 0$) while preserving reciprocity ($P_{ext} = 0$). The resulting system is no longer subject to the passivity-based optical-theorem bound of Eq. (6), thereby permitting nonzero magnetoelectric coupling in the absence of electric and magnetic polarizabilities and enabling the realization of a purely bianisotropic response.

An additional insight follows from Eq. (7). Since reciprocity enforces $P_{ext} = 0$, in the purely bianisotropic limit, the power balance requires $P_{abs} = -P_{sca}$ meaning the power radiated by the induced dipoles must be supplied internally. Thus, realizing a purely bianisotropic response necessitates operation at the loss-compensation point, where optical gain exactly balances dissipative and radiative losses. At this threshold, finite magnetoelectric coupling is sustained with no net power exchange with the incident field. Excess gain would drive the system into an amplifying regime $P_{ext} < 0$, while insufficient gain leaves it in a passive lossy state $P_{ext} > 0$, where passivity constraints forbid the purely bianisotropic response. This loss-compensation condition is therefore crucial for realizing a nearly pure bianisotropic response in lossy systems.

Loss-Compensated Plasmonic Nanoshell Dimer

This section presents the design of a subwavelength scatterer exhibiting a nearly pure bianisotropic response at optical frequencies. Following the design methodology explained in[6], such a response can be realized using two closely spaced, nonmagnetic subwavelength particles whose individual electric polarizabilities, $\boldsymbol{\alpha}_{ee}^{(1)}$ and $\boldsymbol{\alpha}_{ee}^{(2)}$, have real parts of equal magnitude and opposite sign, $\mathbf{Re}(\boldsymbol{\alpha}_{ee}^{(1)}) = -\mathbf{Re}(\boldsymbol{\alpha}_{ee}^{(2)})$, and negligible imaginary parts. Under these conditions, the effective electric polarizability is suppressed, while the magnetic polarizability remains negligible due to the nonmagnetic nature of the constituents. The response is therefore governed by the magnetoelectric coupling terms, resulting in a predominantly bianisotropic behavior.

In the present work, these conditions are realized using two geometrically asymmetric plasmonic nanoshells with dielectric cores. Owing to their geometric asymmetry, the two nanoshells exhibit slightly detuned plasmonic resonance frequencies. For plasmonic nanoshells, the real part of the electric polarizability changes sign across resonance: it is positive below resonance and negative above. Consequently, a spectral region exists where one particle operates below resonance while the other operates above, allowing a wavelength to be identified where $\mathbf{Re}(\boldsymbol{\alpha}_{ee}^{(1)}) = -\mathbf{Re}(\boldsymbol{\alpha}_{ee}^{(2)})$. In contrast to the lossless realization considered in[6], the proposed plasmonic nanoshells are intrinsically lossy due to both dissipative and radiative losses, resulting in non-negligible imaginary components of their electric polarizabilities, $\mathbf{Im}(\boldsymbol{\alpha}_{ee}^{(1)})$ and $\mathbf{Im}(\boldsymbol{\alpha}_{ee}^{(2)})$. Satisfying only the real-part condition is therefore insufficient to suppress the effective electric response and does not guarantee a nearly pure bianisotropic state. As established in the previous section, achieving a purely bianisotropic response in a lossy scatterer requires operation at the loss-compensation point, $\boldsymbol{P_{ext} = 0}$, where radiative and dissipative losses are fully compensated. Since the extinction power is directly related to the imaginary part of the effective electric polarizability, this condition is physically equivalent to the suppression of the net imaginary part, $\mathbf{Im}(\boldsymbol{\alpha_{ee}}) = \mathbf{0}$. To achieve this regime, optical gain is introduced into the dielectric cores of the plasmonic nanoshells, driving the system toward $\boldsymbol{P_{ext} = 0}$ at the wavelength where the real-part cancellation condition is simultaneously satisfied.

`

Several strategies can be envisioned to achieve this loss compensation. One approach is to introduce optical gain into the core of only one plasmonic nanoshell while keeping the second particle passive and lossy. In this configuration, the gain-assisted particle is driven into the spasing regime[10], resulting in a negative imaginary part of its electric polarizability, $\mathrm{Im}(\alpha_{ee}^{(1)}) < 0$, which compensates for the positive imaginary part of the lossy particle, $\mathrm{Im}(\alpha_{ee}^{(2)}) > 0$, in the spectral region where the real-part cancellation condition holds. Such a gain–loss configuration has been explored in PT-symmetric plasmonic dimers with balanced gain and loss[13], in loss-compensation-symmetry dimers where the gain and loss are unbalanced[14], and in a microwave realization of a shadow-free scatterer using active and passive lumped elements[7]. Although this approach can, in principle, achieve the required loss compensation, it demands precise balancing of the gain and loss contributions and is prone to instabilities in the emissive regime[7,14], where the linear gain model fails, and a full dynamical description based on the optical Bloch equations becomes necessary[10]. In this work, we adopt an alternative strategy: optical gain is introduced into the dielectric cores of both plasmonic nanoshells and tuned to compensate their combined dissipative and radiative losses. In this regime, neither particle operates beyond the spasing threshold. Instead, the imaginary parts of the individual polarizabilities are minimized at the design wavelength, $\mathrm{Im}(\alpha_{ee}^{(1)}), \mathrm{Im}(\alpha_{ee}^{(2)}) \approx 0$. This approach enables operation near the loss-compensation point while maintaining a stable, predominantly bianisotropic scattering response.

Electric Polarizability of a Gain-Assisted Plasmonic Nanoshell. The dipolar electric polarizability of a gain-assisted plasmonic nanoshell, shown in Fig. 1(a), consisting of a gain-doped dielectric core of radius r_1 with permittivity ε_g and a metallic shell of outer radius r_2 with permittivity ε_m, embedded in a host medium with permittivity ε_h, is given by the standard analytical expression for coated spheres[10,12]:

$$\alpha_0 = 4\pi r_2^2 \varepsilon_h \frac{(\varepsilon_m - \varepsilon_h)(\varepsilon_g - 2\varepsilon_m) + \rho^3(\varepsilon_g - \varepsilon_m)(\varepsilon_h + 2\varepsilon_m)}{(\varepsilon_m + 2\varepsilon_h)(\varepsilon_g + 2\varepsilon_m) + 2\rho^2(\varepsilon_m - \varepsilon_h)(\varepsilon_g - \varepsilon_m)} \tag{8}$$

where $\rho = r_1/r_2$ is the core-shell ratio. This expression provides the quasistatic polarizability of the nanoshell. To obtain the full electrodynamic polarizability α that satisfies the optical theorem Eq. (6), we apply the radiation-reaction correction[4,5]:

$$\frac{1}{\alpha} = \frac{1}{\alpha_0} - \frac{ik^3}{6\pi} \tag{9}$$

This correction accounts for radiative damping and ensures consistency with the optical theorem. The metallic shell is made of silver (Ag), and its complex permittivity is taken from the experimental data of Johnson and Christy[15]. The core consists of gain-doped silica, providing optical gain tuned to achieve the loss-compensation condition required to approach the nearly pure bianisotropic regime. The gain medium is modeled using a simplified effective-medium description, where the permittivity is expressed as $\varepsilon_g = (n_g + ik_g)^2$, with $n_g = 1.46$ and $k_g < 0$ representing optical gain. The gain coefficient k_g is treated as a tunable quantity and is adjusted to enforce the loss-compensation condition at the design wavelength.

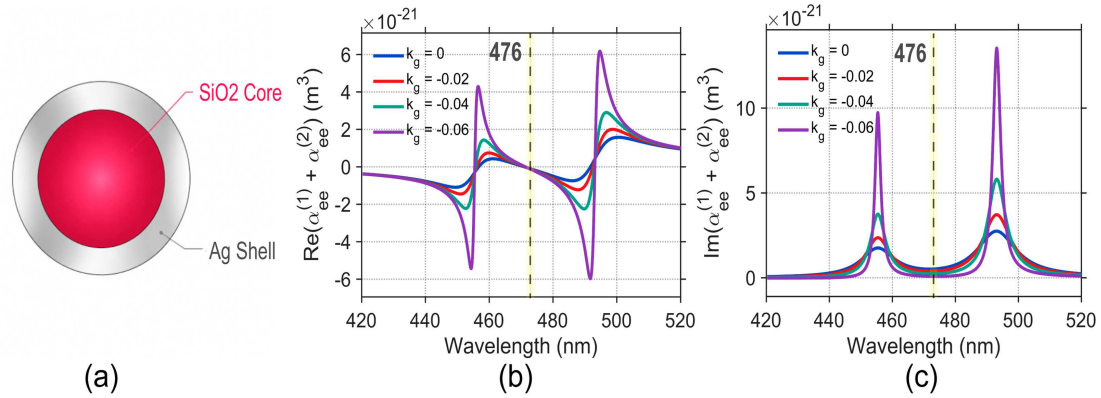


Fig. 1. (a) Schematic of a nanoshell with a gain-doped silica core and a silver shell. (b) Real and (c) imaginary parts of the quantity $\alpha_{ee}^{(1)} + \alpha_{ee}^{(2)}$ for different values of the gain coefficient k_g.

`

Nanoshell Dimer Design. Having established the design methodology and the polarizability of a single gain-assisted plasmonic nanoshell, we now introduce the proposed dimer configuration. The system consists of two closely spaced nanoshells embedded in air and excited by an x-polarized plane wave propagating along the dimer axis (z-axis), as illustrated in Fig. 2(a). As a representative design, the first nanoparticle has inner and outer radii $r_1^1 = 15$ nm and $r_2^1 = 20$ nm, respectively, while the second nanoparticle has $r_1^2 = 20$ nm and $r_2^2 = 25$ nm. These parameters introduce controlled geometric asymmetry through different core–shell ratios, ρ_1 and ρ_2, leading to a slight detuning of their plasmonic resonances while preserving the spectral proximity required for effective coupling. With a subwavelength separation of $d = 30$ nm, the particles interact through their near fields, giving rise to a coupled electromagnetic system. Owing to the structural asymmetry, mutual coupling, and the orientation of the particle pair with respect to the incident field, the system exhibits an omega-type bianisotropic response, described as:

$$\begin{aligned} p_x &= \alpha_{ee}^{xx} E_x + \alpha_{em}^{xy} H_y \\ m_y &= \alpha_{me}^{yx} E_x + \alpha_{mm}^{yy} H_y \end{aligned} \tag{10}$$

For this design, the magnetic polarizability α_{mm}^{yy} is expected to be naturally weak due to the use of nonmagnetic materials. Metallic nanoparticles do not support intrinsic magnetic dipole responses at optical frequencies, and the silica cores are far from their magnetic Mie resonance at the design wavelength. As a result, achieving a purely bianisotropic response depends primarily on the suppression of the electric polarizability, α_{ee}^{xx}, while simultaneously sustaining the magnetoelectric coupling terms, α_{em}^{xy} and α_{me}^{yx}. To illustrate the cancellation mechanism discussed earlier, we calculate the individual electric polarizabilities of the two nanoshells using Eq. (9). Figure 1(b) and 1(c) show the real and imaginary parts of the quantity $\alpha_{ee}^{(1)} + \alpha_{ee}^{(2)}$ for different values of the gain coefficient k_g. It is important to emphasize that this quantity is shown for illustrative purposes only; it represents the sum of the individual polarizabilities and does not correspond to the effective polarizability of the coupled dimer. Nevertheless, it clearly demonstrates that the real parts cancel $\mathrm{Re}(\alpha_{ee}^{(1)}) = -\mathrm{Re}(\alpha_{ee}^{(2)})$ near 476 nm, while the imaginary parts, initially significant due to plasmonic losses, are progressively reduced as gain increases and approach zero for $k_g = -0.06$ at the same wavelength. This simultaneous cancellation of the real parts and suppression of the imaginary parts indicates that the loss-compensation condition can be satisfied, and hence a nearly pure bianisotropic response is theoretically possible near 476 nm.

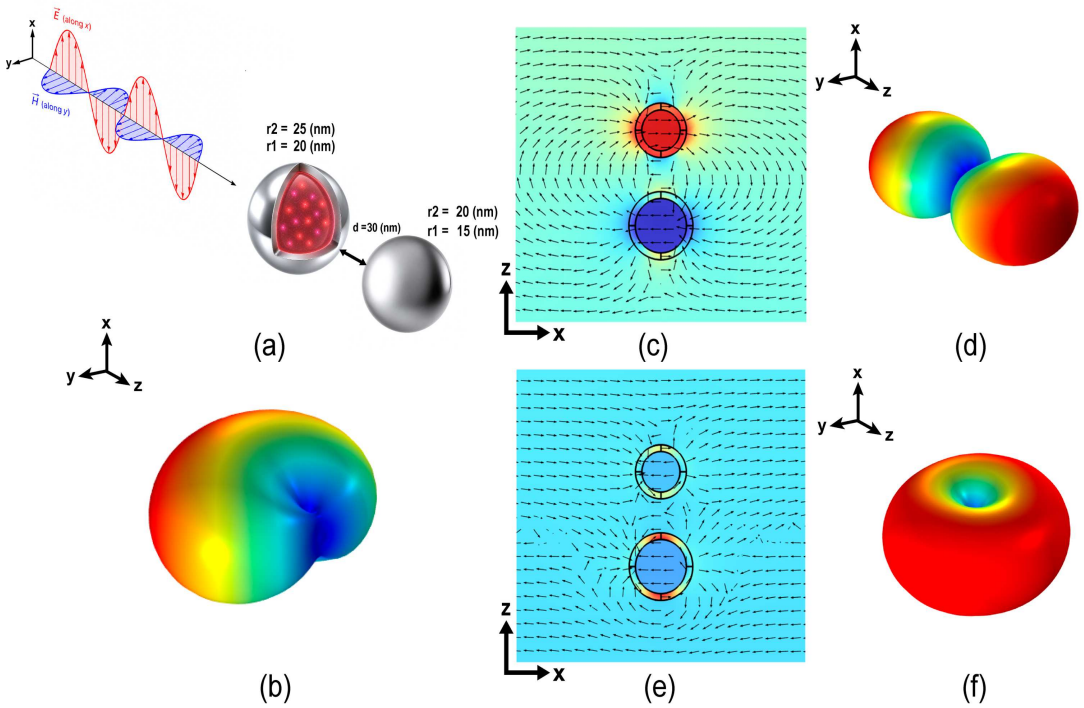


Fig. 2. (a) Schematic of the proposed plasmonic nanoshell dimer. (b) Far-field scattering pattern of the dimer under plane-wave illumination at 479 nm for $k_g = -0.06$. Current density distribution and far-field scattering pattern at 479 nm and for $k_g = -0.06$ under (c, d) electric-field and (e, f) magnetic-field excitation.

`

Simulation Results and Discussion. To confirm the predictions of the cancellation mechanism and to quantitatively validate the nearly pure bianisotropic response, full-wave electromagnetic simulations were performed using the finite-element solver COMSOL Multiphysics. The direct and indirect coupling coefficients of the coupled dimer were obtained using the dipole retrieval procedure explained in[16]. Figure 3(a) shows the magnitudes of the extracted polarizabilities for different values of the gain coefficient k_g. In the absence of gain ($k_g = 0$), the electric polarizability α_{ee}^{xx} is comparable in magnitude to the electromagnetic polarizability, preventing the system from exhibiting a predominantly bianisotropic response. As the gain level increases, the magnitude of the electric polarizability decreases progressively due to the suppression of dissipative and radiative losses. For $k_g = -0.06$, the electric polarizability is reduced by approximately three orders of magnitude relative to the electromagnetic polarizability at the wavelength of 479 nm. To quantify the degree of bianisotropy, we use the dimensionless bianisotropy factor $\Gamma_b = \sqrt{|\alpha_{em}\alpha_{me}|}/\sqrt{|\alpha_{ee}\alpha_{mm}|}$, which characterizes the relative strength of the indirect magnetoelectric coupling coefficients compared to the direct electric and magnetic ones. Figure 3(b) shows the evolution of Γ_b for different gain values. For $k_g = -0.06$, the indirect coupling terms exceed the direct ones by a factor of approximately 110 near 479 nm. The real and imaginary parts of the retrieved polarizabilities for $k_g = -0.06$ are shown in Figs. 3(c) and 3(d). Figure 3(c) demonstrates that the real part of the electric polarizability crosses zero near 479 nm, consistent with the cancellation of the electric polarizabilities of the two detuned nanoshells. Moreover, its imaginary part is simultaneously suppressed through the loss compensation mechanism. In contrast, Fig. 3(d) shows that the electromagnetic polarizability remains finite in the same spectral region. These simulation results confirm that the nearly pure bianisotropic response is achieved at 479 nm for $k_g = -0.06$, in good agreement with the theoretical prediction of 476 nm.

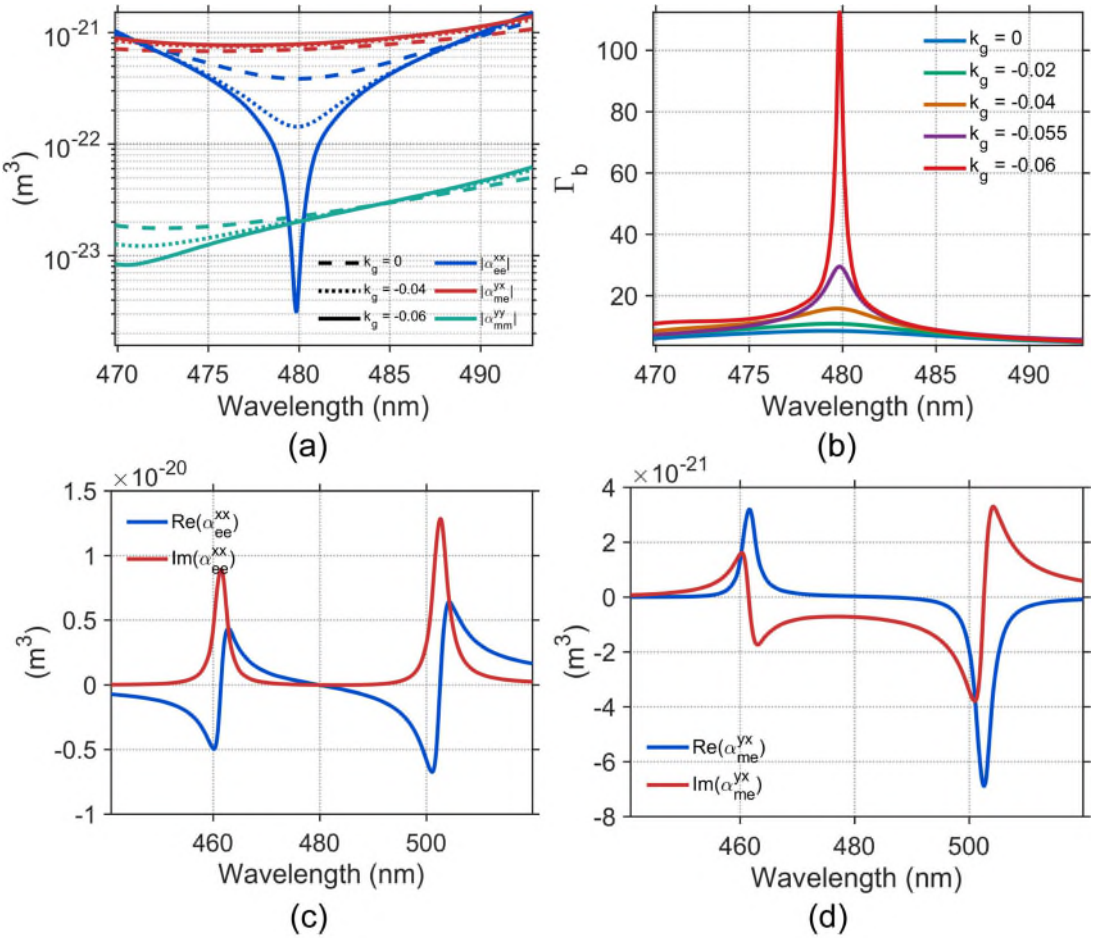


Fig. 3. (a) Magnitudes of the polarizabilities α_{ee}^{xx} (blue), α_{me}^{yx}(red), and α_{mm}^{yy}(green) for different values of the gain coefficient k_g. (b) Evolution of the bianisotropy factor Γ_b for different gain values. Real and imaginary parts of the retrieved (c) electric polarizability α_{ee}^{xx} and (d) electromagnetic polarizability α_{me}^{yx} for $k_g = -0.06$.

`

Achieving the loss-compensation condition for this structure is further evidenced in Fig. 4(a), which shows the scattering, extinction, and absorption cross sections at 479 nm, as a function of the gain coefficient k_g. As k_g approaches -0.06, σ_{ext} decreases to zero and σ_{abs} becomes negative, indicating that optical gain overcomes the dissipative and radiative losses. The scattering cross section remains moderate, reflecting scattering through the magnetoelectric coupling terms. To directly connect these observations to the underlying polarizabilities, Fig. 4(b) shows the imaginary parts of the extracted polarizabilities at 479 nm as a function of k_g. The imaginary part of the electric polarizability, $\mathrm{Im}(\alpha_{ee}^{xx})$, decreases to zero, while the imaginary part of the magnetoelectric polarizability remains finite. This confirms that the loss-compensation condition is achieved through the suppression of $\mathrm{Im}(\alpha_{ee}^{xx})$, in agreement with the theoretical framework established earlier.

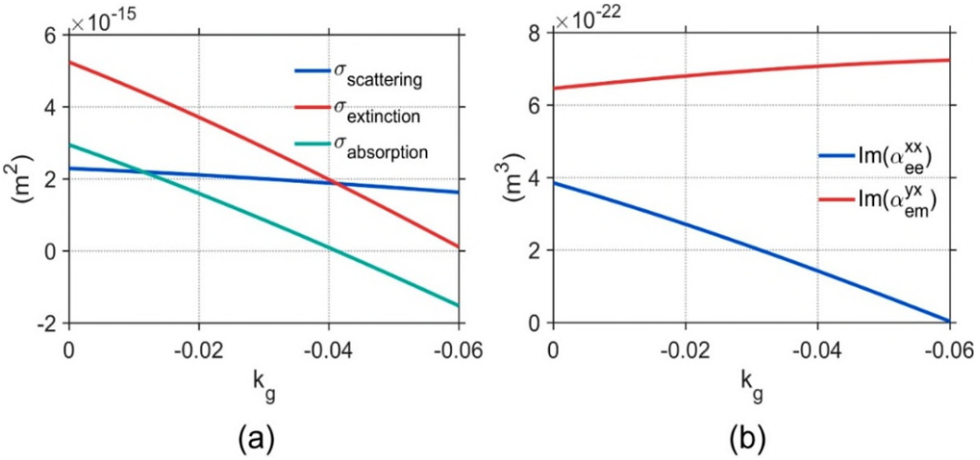


Fig. 4. (a) Scattering, extinction, and absorption cross sections at 479 nm as a function of the gain coefficient k_g. (b) Imaginary part of electric and magnetoelectric polarizability at 479 nm as a function of k_g.

To further demonstrate the microscopic origin of the magnetoelectric coupling coefficients and the suppression of the electric and magnetic polarizabilities, we excite the dimer using two counter-propagating plane waves. By adjusting their relative phase, two distinct excitation conditions can be realized. In the first case, the relative phases are adjusted so that the magnetic fields interfere destructively at the center of the dimer ($H = 0$), while the electric fields interfere constructively. Under this pure electric-field excitation, the induced electric dipole moments in the two particles are equal in magnitude but opposite in direction ($p_1 = -p_2$), resulting in a strongly suppressed net electric dipole moment ($p_x = \alpha_{ee}^{xx} E_x \approx 0$). However, the antiparallel dipole configuration produces a circulating current distribution, giving rise to an effective magnetic dipole moment along the y-axis, associated with the electromagnetic polarizability ($m_y \approx \alpha_{me}^{yx} E_x$), as illustrated in Fig. 2(c). The corresponding far-field scattering pattern at 479 nm, given in Fig. 2(d), exhibits interference between this magnetic dipole and an electric quadrupole arising from the finite spatial separation of the antiparallel electric dipoles. Conversely, when the electric fields interfere destructively at the center of the dimer ($E = 0$), while the magnetic fields interfere constructively, the circulating electric field induced via Faraday's law excites electric dipole moments in the two particles that are aligned in the same direction along the x-axis, resulting in a finite electric dipole moment associated with the magnetoelectric polarizability ($p_x \approx \alpha_{em}^{xy} H_y$), as shown in Fig. 2(e). In contrast, the magnetic dipole moment is negligible ($m_y = \alpha_{mm}^{yy} H_y \approx 0$), consistent with the nonmagnetic nature of the constituent particles. The corresponding far-field scattering pattern, shown in Fig. 2(f), exhibits the characteristic doughnut-shaped profile of an electric dipole at 479 nm. These results confirm that the direct electric and magnetic responses are suppressed while the magnetoelectric coupling terms remain finite, consistent with the polarizability retrieval in Fig. 3.

Dispersive Gain Model and Practical Feasibility

In the last section, the gain medium was modeled using a simplified effective-medium description with a constant complex permittivity. This constant-gain approximation, while widely employed in conceptual studies of gain-assisted plasmonic systems[11,12], neglects the frequency dispersion and saturation inherent to realistic

`

gain media. However, this approximation is justified for the present conceptual demonstration because the system operates below the lasing threshold, and gain is required only within a narrow spectral window around the design wavelength where the real-part cancellation and loss-compensation conditions are simultaneously satisfied. Nevertheless, to verify the robustness of our conclusions, we also performed simulations using a dispersive Lorentzian gain model as described in[10]. Using this model, the gain permittivity is described by a Lorentzian lineshape centered at the design wavelength, with parameters chosen to match the constant-gain value $k_g = -0.06$ at 479 nm (the gain coefficient obtained from the dispersive model is shown in Fig. 5(a)). The same simulations were performed using this dispersive model, and the bianisotropy factor obtained from the dispersive model is shown in Fig. 5(b), confirming that the nearly pure bianisotropic response is robust to realistic gain dispersion and is not an artifact of the constant-gain approximation.

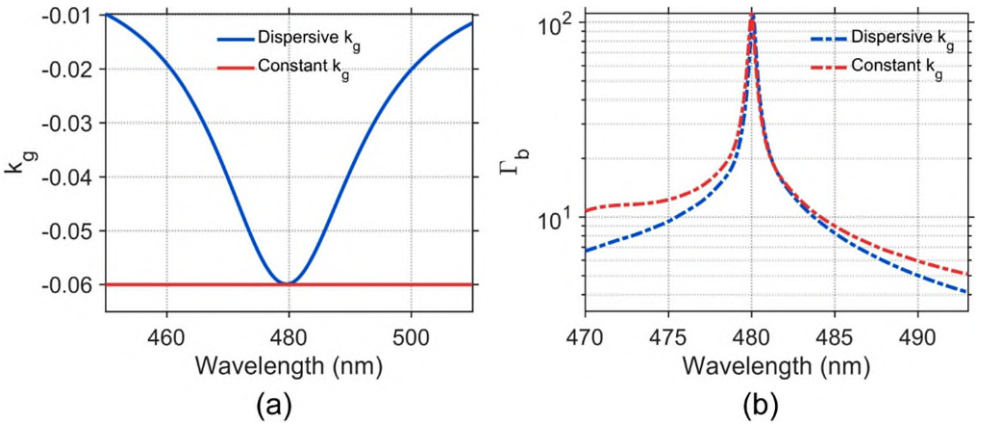


Fig. 5. (a) Gain coefficient k_g as a function of wavelength for the constant gain model (red) and the dispersive Lorentzian gain model (blue). (b) Bianisotropy factor as a function of wavelength obtained by the constant and dispersive gain models.

To further evaluate the experimental feasibility of the proposed dimer, we assess the magnitude of the required gain coefficient. The gain coefficient $k_g = -0.06$ corresponds to an amplification coefficient of light intensity $g = -4\pi k_g/\lambda \approx 1.57 \times 10^4 \mathrm{cm}^{-1}$ at $\lambda = 479$ nm. This amplification coefficient can be expressed as $g = N\sigma_e$, where N is the gain concentration and σ_e is the emission cross-section of the gain material. Achieving such a high gain coefficient typically requires both a large emission cross-section and a high concentration. This requirement has been explored in conceptual studies of gain-assisted plasmonic systems, where gain coefficients up to $k_g = -0.2$ have been investigated theoretically and numerically[11,12,17,18]. These works have considered organic dyes, rare-earth ions, and quantum dot inclusions as potential gain media. However, none of these studies address a specific physical material that can satisfy such high gain values experimentally. Nevertheless, experimental demonstrations of comparable gain coefficients do exist. For instance, T5oCx films[18,19] have demonstrated a gain coefficient up to $k_g = -0.123$ at 610 nm (corresponding to $g = 2.53 \times 10^4 \mathrm{cm}^{-1}$), and gain coefficients up to $g = 6.8 \times 10^4 \mathrm{cm}^{-1}$ have been achieved using quantum dot inclusions at cryogenic temperatures[18,20]. Additionally, loss compensation has been experimentally verified in OG-488 dye-doped silica shells within a core-shell spaser geometry[21] at 531 nm. These results show that gain coefficients of the required order are experimentally attainable, although none provide the exact gain coefficient required near the design wavelength of 479 nm. Thus, the direct realization of our specific structure remains a challenge that requires further investigation. As a step toward addressing this challenge, we suggest possible pathways for a practical realization. First, the operating wavelength of the nearly pure bianisotropic response can be tuned by adjusting the nanoshell dimer geometry. Changing the core radii shifts the response across most of the visible spectrum, allowing it to match the excitation window of available gain media. For example, core radii of 15 nm and 20 nm with a 5 nm silver shell yield a predominantly bianisotropic response at 479 nm for $k_g = -0.06$, whereas increasing the core radii to 40 nm and 45 nm shifts the response to 675 nm for $k_g = -0.1$ (corresponding to $g = 1.86 \times 10^4 \mathrm{cm}^{-1}$). Moreover, the required gain coefficient could be reduced by employing alternative nanoparticle geometries (e.g., disk-shaped or nanorod geometries) or different host materials. Thus, while the exact gain values at 479 nm have not been experimentally realized, the concept is physically plausible and provides a practical design framework whose realization will depend on the appropriate selection of a gain medium and nanofabrication.

Scattering Pattern of the Proposed Nanoshell Dimer

The far-field scattering pattern of the proposed nanodimer, evaluated at the nearly pure bianisotropic operating wavelength of 479 nm for the gain coefficient $k_g = -0.06$, is shown in Fig. 2(b). The pattern exhibits

`

suppressed forward scattering and enhanced backward scattering, characteristic of the second Kerker effect[22,23]. This behavior can be explained by the fact that at this wavelength the response of the nanodimer is governed by electric and magnetic dipole moments arising almost exclusively from magnetoelectric coupling, i.e., $p_x \approx \alpha_{em}^{xy} H_y, m_y \approx \alpha_{me}^{yx} E_x$. Due to reciprocity, $\alpha_{em}^{xy} = -\alpha_{me}^{yx}$, the induced moments are equal in magnitude but out of phase, thereby satisfying the second Kerker condition. To further quantify this directional scattering behavior, we compute the nanodimer's radar scattering cross-section, shown in Fig. 6. The far-field scattered electric field of a dipolar scatterer is given by

$$E_{sca}(r) = \frac{k^2}{4\pi r} e^{ikr}[(\hat{n} \times p) \times \hat{n} - \hat{n} \times m] \tag{11}$$

where $\hat{n}$ is the unit vector in the scattering direction. Using Eq. (11), the scattering cross sections in the forward ($\theta = 0$) and backward ($\theta = \pi$) directions are obtained as

$$\sigma_f = \lim_{r\to\infty} 4\pi r^2 \frac{|E_{sca}(\varphi = 0, \theta = 0)|^2}{|E_{inc}|^2} = \frac{k^4}{4\pi}\left|\alpha_{ee}^{xx} + \alpha_{em}^{xy} + \alpha_{me}^{yx} - \alpha_{mm}^{yy}\right|^2 \tag{12}$$

$$\sigma_b = \lim_{r\to\infty} 4\pi r^2 \frac{|E_{sca}(\varphi = 0, \theta = \pi)|^2}{|E_{inc}|^2} = \frac{k^4}{4\pi}\left|\alpha_{ee}^{xx} - \alpha_{em}^{xy} + \alpha_{me}^{yx} - \alpha_{mm}^{yy}\right|^2 \tag{13}$$

In the nearly pure bianisotropic regime, where $\alpha_{ee}^{xx} \approx 0$ and $\alpha_{mm}^{yy} \approx 0$, the forward scattering cross section vanishes ($\sigma_f \approx 0$) due to reciprocity, $\alpha_{em}^{xy} = -\alpha_{me}^{yx}$, while the backward scattering remains finite ($\sigma_b \approx \frac{k^4}{4\pi}\left|\alpha_{me}^{yx}\right|^2$) and is enhanced due to constructive interference of the magnetoelectric contributions.

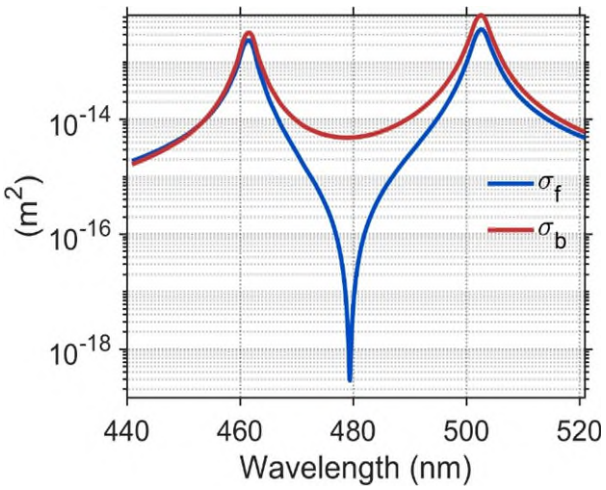


Fig. 6. Forward (σ_f) and backward (σ_b) radar scattering cross sections as a function of wavelength.

Another unconventional scattering response emerges when the nanodimer is reoriented in the plane of the incident field with a larger inter-particle separation, depicted in Fig. 7(a). At 477 nm and for the gain coefficient $k_g = -0.06$, the induced electric dipole moments in the two nanoshells are equal in magnitude but opposite in phase, resulting in a strongly suppressed net electric dipole moment. In this configuration, the system sustains a net magnetic dipole moment oriented along the z-axis, accompanied by an electric quadrupole contribution due to the finite separation of the particles. The extracted dipole moments, plotted in Fig. 8(a), confirm that the magnetic dipole dominates at 477 nm. Consequently, the far-field scattering pattern in Fig. 7(b) is governed by the interference between the magnetic dipole and the electric quadrupole, giving rise to predominantly lateral scattering. This side-scattering response can be further engineered to achieve directional lateral scattering by introducing an additional passive nanoshell between the two particles, as illustrated in Fig. 7(c). The central particle, with radii $r_1^3 = 17.5\ nm$ and $r_2^3 = 22.5\ nm$, is chosen as the geometrical mean of the outer particles to position its plasmonic resonance near 480 nm. This particle is kept passive ($k_g = 0$) so that its induced electric dipole moment is comparable in magnitude to the magnetic dipole moment of the gain-assisted dimer at the operating wavelength.

`

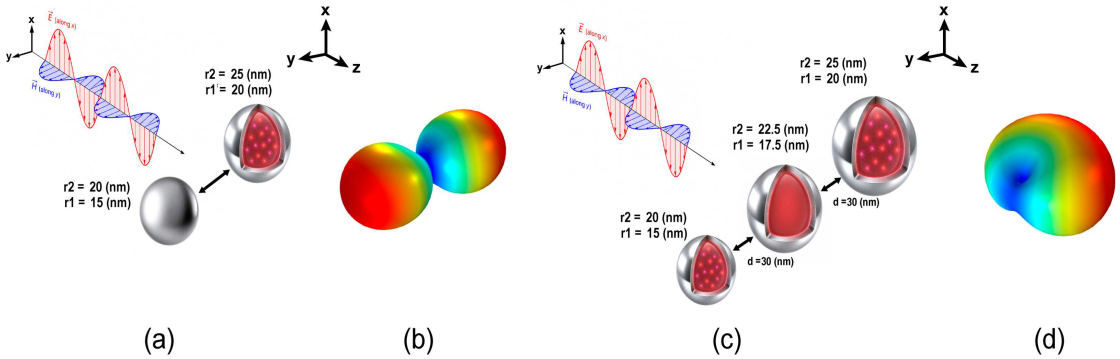


Fig. 7. (a) Schematic of the nanodimer reoriented in the plane of the incident field. (b) Far-field scattering pattern at 477 nm for $k_g = -0.06$, showing predominantly lateral scattering. (c) Schematic of the trimer, the proposed dimer with an additional passive nanoshell located in between. (d) Far-field scattering pattern of the trimer at 477 nm, showing highly directional lateral scattering along the $-y$ direction.

By tuning the inter-particle spacing, the electric and magnetic dipole moments are matched at 477 nm, as confirmed in Fig. 8(b). Under this condition, the trimer supports strong magnetoelectric interference, producing highly directional lateral scattering with radiation predominantly directed along the $-y$, as depicted in Fig. 7(c). This directionality arises from the interference between the magnetic dipole of the dimer (oriented along z) and the electric dipole of the central particle (oriented along x).

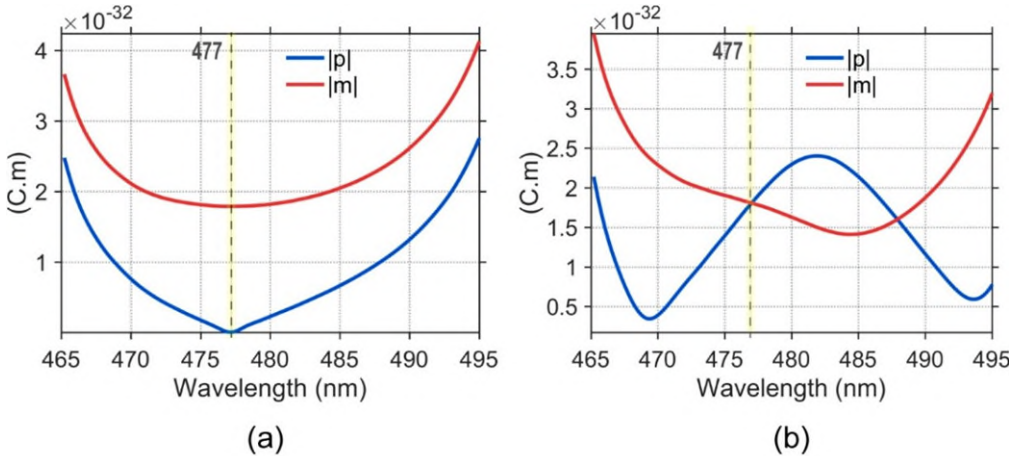


Fig. 8. Magnitudes of the electric and magnetic dipole moments induced by the (a) dimer and (b) trimer.

Conclusion

In this work, we established the conditions required to realize a purely bianisotropic response in reciprocal lossy systems. We showed that the optical theorem prohibits passive reciprocal scatterers from simultaneously suppressing the direct electric and magnetic polarizabilities while preserving finite magnetoelectric coupling, and that this limitation can be overcome at a loss-compensation point where dissipative and radiative losses are balanced by optical gain. Based on this principle, we proposed a loss-compensated plasmonic nanoshell dimer in which resonance detuning suppresses the net electric dipole response while optical gain compensates the intrinsic losses. Full-wave simulations confirmed a nearly pure bianisotropic response at visible frequencies, with the magnetoelectric polarizabilities exceeding the direct electric and magnetic polarizabilities by more than two orders of magnitude. We further showed that this regime enables near-complete forward-scattering suppression and highly directional lateral scattering through magnetoelectric interference. These results establish a general framework for engineering nearly pure bianisotropic scatterers in active nanophotonic systems and may provide new opportunities for directional light manipulation and active metasurface design.

Data availability

Data underlying the results presented in this paper are available from the corresponding author upon reasonable request.

References

1. Poleva, M. et al. Multipolar theory of bianisotropic response of meta-atoms. *Phys. Rev. B* **107**, L041304 (2023).

`

2. Alaee, R., Rockstuhl, C. & Fernandez-Corbaton, I. Exact multipolar decompositions with applications in nanophotonics. *Adv. Opt. Mater.* **7**, 1800783 (2019).
3. Alaee, R. et al. All-dielectric reciprocal bianisotropic nanoparticles. *Phys. Rev. B* **92**, 245130 (2015).
4. Sersic, I., Tuambilangana, C., Kampfrath, T. & Koenderink, A. F. Magneto-electric point scattering theory for metamaterial scatterers. *Phys. Rev. B* **83**, 245102 (2011).
5. Kolkowski, R. & Koenderink, A. F. Lattice resonances in optical metasurfaces with gain and loss. *Proc. IEEE* **108**, 795-818 (2020).
6. Albooyeh, M. et al. Purely bianisotropic scatterers. *Phys. Rev. B* **94**, 245428 (2016).
7. Safari, M., Albooyeh, M., Simovski, C. R. & Tretyakov, S. A. Shadow-free multimers as extreme-performance meta-atoms. *Phys. Rev. B* **97**, 085412 (2018).
8. Alaee, R. et al. Magnetoelectric coupling in nonidentical plasmonic nanoparticles: Theory and applications. *Phys. Rev. B* **91**, 115119 (2015).
9. Grahn, P., Shevchenko, A. & Kaivola, M. Electric dipole-free interaction of visible light with pairs of subwavelength-size silver particles. *Phys. Rev. B* **86**, 035419 (2012).
10. Caicedo, K. et al. Gain-driven singular resonances in active core-shell and nano-shell plasmonic particles. *J. Opt. Soc. Am. B* **39**, 107-115 (2022).
11. Singh, A. K., Pal, S. & Ghosh, S. Engineering chiral plasmonic nanostructures for gain-assisted plasmon amplification and tunable enhancement of circular dichroism. *Mater. Adv.* **3**, 1825-1833 (2022).
12. Wang, Q., Pan, S., Guo, Y., Li, Z. & Liu, J. Plasmonic effect of a nanoshell dimer with different gain materials. *Plasmonics* **9**, 1463-1469 (2014).
13. Klimov, V. & Lupu, A. Entanglement of bright and dark modes in parity-time-symmetric plasmonic nanoantennas. *Phys. Rev. B* **100**, 245434 (2019).
14. Klimov, V. V., Zabkov, I. V., Guzatov, D. V. & Vinogradov, A. P. Loss compensation symmetry in dimers made of gain and lossy nanoparticles. *Laser Phys. Lett.* **15**, 035901 (2018).
15. Johnson, P. B. & Christy, R. W. Optical constants of the noble metals. *Phys. Rev. B* **6**, 4370-4379 (1972).
16. Asadchy, V. S., Faniayeu, I. A., Ra'di, Y. & Tretyakov, S. A. Determining polarizability tensors for an arbitrary small electromagnetic scatterer. *Photon. Nanostruct.* **12**, 298-304 (2014).
17. Song, J. et al. Ultrahigh enhancement factor by using a silver nanoshell with a gain core above a silver substrate for surface-enhanced Raman scattering at the single-molecule level. *IEEE Photonics J.* **7**, 4501508 (2015).
18. Li, Z.-Y. & Xia, Y. Metal nanoparticles with gain toward single-molecule detection by surface-enhanced Raman scattering. *Nano Lett.* **10**, 243-249 (2010).
19. Pisignano, D. et al. Amplified spontaneous emission and efficient tunable laser emission from a substituted thiophene-based oligomer. *Appl. Phys. Lett.* **81**, 3534 (2002).
20. Kirstaedter, N. et al. Gain and differential gain of single layer InAs/GaAs quantum dot injection lasers. *Appl. Phys. Lett.* **69**, 1226-1228 (1996).
21. Noginov, M. A. et al. Demonstration of a spaser-based nanolaser. *Nature* **460**, 1110-1112 (2009).
22. Kerker, M., Wang, D.-S. & Giles, C. L. Electromagnetic scattering by magnetic spheres. *J. Opt. Soc. Am.* **73**, 765-767 (1983).
23. Liu, W. & Kivshar, Y. S. Generalized Kerker effects in nanophotonics and meta-optics [Invited]. *Opt. Express* **26**, 13085-13105 (2018).

Author contributions

M.S. conceived the idea, developed the theoretical framework, performed the numerical simulations, and wrote the manuscript. A.N. and H.O. supervised the project and reviewed the manuscript.

Funding Declaration

This research received no external funding.

Competing interests

The authors declare no competing interests.

Additional information

Correspondence and requests for materials should be addressed to A.N.

`